Biophysical Journal, Volume *114*

Supplemental Information

ECM Cross-Linking Regulates Invadopodia Dynamics

Kamyar Esmaeili Pourfarhangi, Aviv Bergman, and Bojana Gligorijevic

Model description

The mathematical model was developed based on the following assumptions and can be applied to any dimensionality of ECM architecture:

1. Average concentration of growth factor stimuli and intact, non-degraded ECM is assumed to be constant in the system;
2. High ECM concentration and crosslinking ratio can create physical barriers, inhibiting cell migration through the ECM (1, 2);
3. ECM degradation rate is assumed to exponentially decrease as ECM concentration is depleted (exponential decay);
4. The potential of the cell for ECM degradation is assumed to decay between two cycles of MMP delivery (3);
5. It is assumed that cells migrate in a constant speed in a condition when there is no physical barrier opposing the cell movement.

The sets of ordinary differential equations predicting the changes in these three variables are as follows:

$$\frac{dC_{ECM}}{dt} = K_a * M * C_{ECM}^2 \left({(C_{ECM}^* - C_{ECM})} \Big/ {(1+X)^n C_{ECM}^*} \right) - K_c\, I \left(1 - exp(-K_{ic} C_{ECM})\right) \quad \text{(Eq.1)}$$

$$\frac{dI}{dt} = K_{ci}\, I \left(1 - exp(-K_{ic} C_{ECM})\right) - K_i\, I \quad \text{(Eq. 2)}$$

$$\frac{dM}{dt} = K_m ({1}/{(1+X)^n}) V - K_{cm}\, M\, {C_{ECM}}/{C_{ECM}^*} \quad \text{(Eq. 3)}$$

The first term of Equation 1 captures the increase in the ECM concentration when a cell moves from an area where ECM was degraded to an area with high abundance of intact ECM. Hence, the extent of the migration (*M*) has a direct positive effect on the increase in the local ECM concentration. As the migration requires cell-ECM adhesions to be created in the cell front and dissociated at the cell rear (4), dependence of cell migration to cell-ECM adhesions will be nonlinear (5). To capture the non-linear role of adhesions, M is multiplied by $K_a C^2_{ECM}$. Next, increase in ECM concentration and cross-linking ratio will reduce the cell movement by reducing ECM pore size (1, 2). To introduce this hindering effect to Equation 1, the first term of this equation is multiplied by $\left({(C_{ECM}^* - C_{ECM})} \Big/ {(1+X)^n C_{ECM}^*} \right)$. Higher ECM concentration and cross-linking ratio decrease the value of this term, therefore decreasing the total value of the whole Equation 1 (dC_{ECM}/dt). In this term, exponent *n* is a constant dependent on cell and ECM geometry, adapting the equation for various types of ECMs and cells. The exponent *n* captures the non-linear effects of crosslinking in creating physical barriers against cell migration. The value of this exponent was determined experimentally (**Figure S1**). The second term of Equation 1 depicts the degradation rate of the intact ECM by proteolytic activity of invadopodia. It is assumed that ECM degradation would exponentially reduce with the level of intact ECM, due to lesser availability of non-degraded ECM for proteolysis.

The first term of Equation 2 is the rate at which a cell degrades ECM. The higher the levels of Invadopodia state (I) and ECM concentration (C_{ECM}), the higher is the rate of invadopodia degradation. In this model, it is assumed that between two protease delivery events, the potential of invadopodia proteolytic activity decreases due to lesser availability of protease molecules (eg.

MT1-MMP). The second term of Equation 2 captures this negative effect on the invadopodia degradation value.

Table S1. List of variables and constants used in the model

Variable/Constant	Description	Unit	Value	reference
C_I	ECM concentration	Dimensionless (Percentage)	100 to 0	NA
C^*_{ECM}	Intact ECM concentration	Dimensionless	100	NA
I	Invasion state abundance	Dimensionless	$I_0 = 1e10^{-6}$	NA
M	Migration state abundance	Dimensionless	$M_0 = 1$	NA
X	ECM crosslinking ratio	Dimensionless	0 to 1	NA
K_a	Cell-ECM adhesion constant	1/s	1	--
K_c	Unit adjusting constant	1/s	1	--
K_{ic}	MT1-MMP proteolysis rate constant	1/s	0.00201	(6)
K_{ci}	Unit adjusting constant	1/s	1	--
K_i	MT1-MMP turnover rate constant	1/s	1/26	(3)
K_m	Unit adjusting constant	1/μm	1	--
K_{cm}	Unit adjusting constant	1/s	1	--
V	Maximum migration speed	μm/s	0.083	(7)
n	Indicator of the ECM cross-linking ratio effect on cell migration	dimensionless	6 for 2D; 7 in 3D assay	This paper **Figure S1**

Equation 3 represents variations in the Migration state levels over time. We assume that each cell has a constant rate of migration in a condition when there is no physical barrier opposing the cell movement. In 2D environment, where there are no physical barriers present on the dorsal side of the cell, the increase in size and number of focal adhesions on the ventral side of the cell can mimic physical barrier. In the first term of Equation 3, this constant speed is denoted by *V*. However, the extent of ECM crosslinking affects this speed. An increase in ECM crosslinking ratio decreases ECM pore size, resulting in a decrease in the velocity of cell migration (2). We assumed that the cell speed non-linearly decreases as the crosslinking ratio increases. The second term of Equation 3 accounts for the physical barriers that ECM concentration is responsible for. As a cell degrades its surrounding ECM, C_{ECM} decreases which causes a decrease in C_{ECM}/C^*_{ECM}, resulting in a decrease in the ECM concentration role in opposing cell migration. The second term is then multiplied by the amount of the Migration state, because it is assumed that the higher the value of the Migration state, the higher are the effects of physical barriers on the cell migration.

The set of ordinary differential equations consisting of Equations 1-3 was simultaneously solved using the kinetic values as indicated in Table 1 and the following initial conditions

$CI_0 = C^*_{ECM} = 100$ (%, intact ECM at the beginning)

$M_0 = 1$

$I_0 = 1e10^{-6}$

M_0 and I_0 are initial values of migration and Invadopodia states. It is assumed that the cell is initially in Migration state, until it reaches a point where it switches to Invadopodia state.

Our model has no spatial terms defined and does not store information about ECM concentration distribution. The model assumes a fixed concentration of intact ECM prior to the arrival of cells with degradation capacity, and that cells always migrate to in the direction where intact ECM is present which in turn stimulates ECM degradation. Such locations can be either in areas not previously visited by the cell or in the vicinity of previously degraded punctae. As a result, new invadopodia assembles and matures and new ECM degradation punctae are formed. If a cell initiates invadopodia assembly at previously degraded punctae, disassembly will occur prior to invadopodia maturation due to the absence of adhesion ligands in the ECM (**Movie S1, S2**).

In regard to ECM role in Migration/Invadopodia oscillations, our model is adhesion-centric. As integrin molecules are well-known mechanosensors, physical forces are likely to influence adhesion strengths and numbers. However, we do not explicitly address physical force effect on the system. Surrogates of the physical force are introduced to the model in the Equation 3, where both increase in cross-linking and concentration of the ECM exert hindering effect towards the abundance of cell migration state (*M*) as well as the maximum migration speed (*V*). For example, the model assumes that when ECM cross-linking is negligible, all cells will "move" at a maximum velocity *V* and these values will both be lower at higher ECM cross-linking and/or concentration levels.

Supporting references:

1. Zaman, M.H., L.M. Trapani, A.L. Sieminski, D. MacKellar, H. Gong, R.D. Kamm, A. Wells, D.A. Lauffenburger, and P. Matsudaira. 2006. Migration of tumor cells in 3D matrices is governed by matrix stiffness along with cell-matrix adhesion and proteolysis. Proc. Natl. Acad. Sci. 103: 10889–10894.
2. Ehrbar, M., A. Sala, P. Lienemann, A. Ranga, K. Mosiewicz, A. Bittermann, S.C. Rizzi, F.E. Weber, and M.P. Lutolf. 2011. Elucidating the role of matrix stiffness in 3D cell migration and remodeling. Biophys. J. 100: 284–293.
3. Hoshino, D., N. Koshikawa, T. Suzuki, V. Quaranta, A.M. Weaver, M. Seiki, and K. Ichikawa. 2012. Establishment and validation of computational model for MT1-MMP dependent ECM degradation and intervention strategies. PLoS Comput. Biol. 8: 1–10.
4. Lauffenburger, D. a, and a L. Horwitz. 1996. Cell migration: A physically integrated process. Cell. 84: 359–369.
5. DiMilla, P.A., K. Barbee, and D.A. Lauffenburger. 1991. Mathematical model for the effects of adhesion and mechanics on cell migration speed. Biophys. J. 60: 15–37.
6. Ohuchi, E., K. Imai, Y. Fujii, H. Sato, M. Seiki, and Y. Okada. 1997. Membrane-Type metalloproteinase digests extracellular matrix macromolecules including interstitial collagens. Matrix Biol. 16: 76–77.
7. Gligorijevic, B., A. Bergman, and J. Condeelis. 2014. Multiparametric Classification Links Tumor Microenvironments with Tumor Cell Phenotype. PLoS Biol. 12.

Supplementary Figures:

Figure S1.

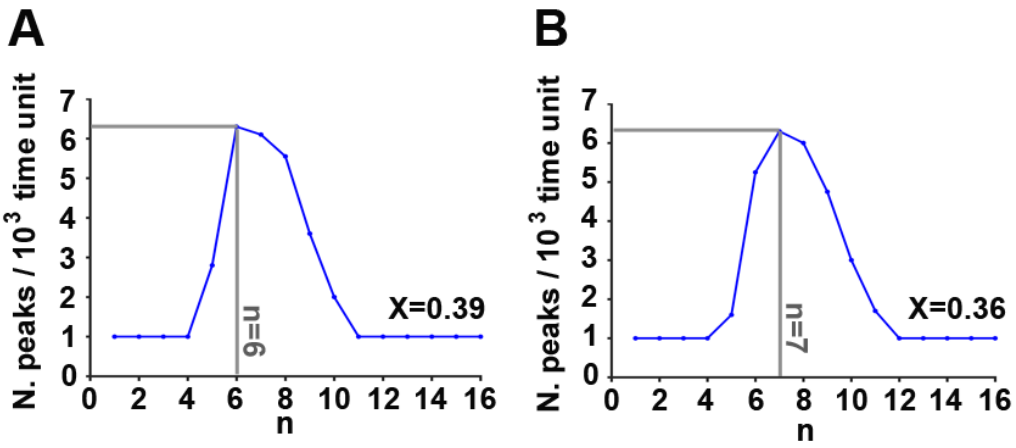

Figure S1. Fitting the value of n to the experimental data. In the model, cross-linking ratio was fixed to the optimal value measured experimentally (0.39 for 2D, 0.36 for 3D). The number of predicted invadopodia/migration switches over time was plotted at different values of n. The value of n with maximal number of switches was chosen, 6 for 2D (**A**) and 7 for the 3D (**B**) conditions.

Figure S2.

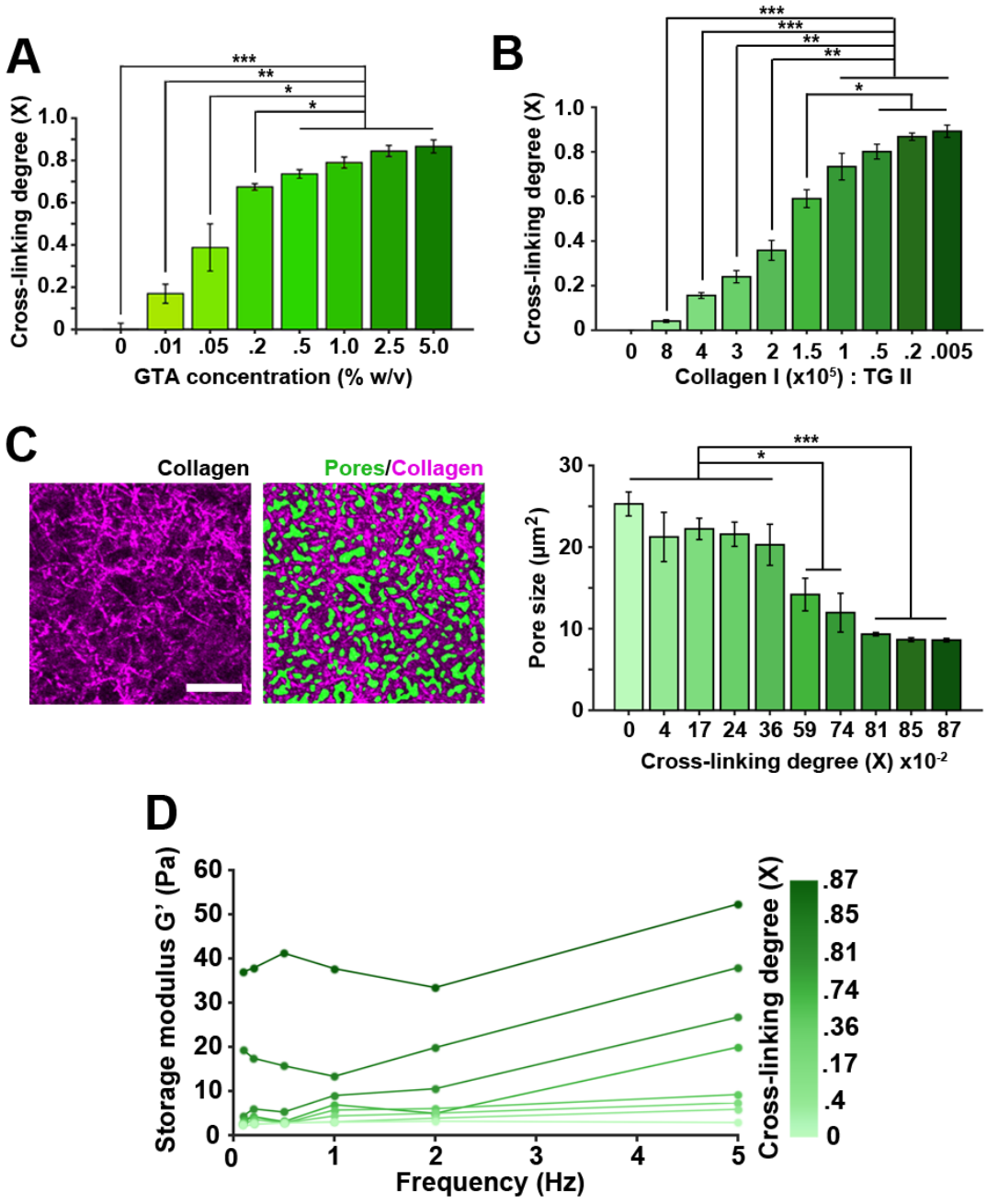

Figure S2. Measurements of physical properties of gelatin and collagen gels: A and B. Increase of the cross-linking ratio of the gelatin (A) and collagen gels (B) with increase in the cross-linker concentration. Errors are shown as SEM. **C.** Images of a representative 3D collagen gel taken by reflection confocal microscopy (raw image, left; processed image, right). Scale bar 5 µm. Bar graph shows pore sizes at different cross-linking degrees. T-test pairwise comparison performed among samples. P<0.05 *, P<0.01 **, P<0.001 *** **D.** Storage modulus of the collagen samples cross-linked with TG II, measured at 0.1-5 Hz frequencies of the strain control test.

Supplementary Movies

Supplementary Movie 1. MTLn3 cell switching from Migration to Invadopodia state.

Time lapse of Cerulean-cortactin-MTLn3 cells (left) cultured on Alexa 488-Gelatin (middle); overlay (right) used for measurements in Figure 1A-D. Centroid tracking is shown in blue and representative invadopodia are marked with red circles (starting 380 and 810 minutes). At the beginning of the movie, cell is migrating across the gelatin layer and assembles short-lived invadopodia precursors. When the cell centroid becomes stationary, the number of ECM-degrading invadopodia increases. Time between frames: 10 minutes. Scale bar is 10 μm.

Supplementary Movie 2. MDA-MB-231 cell switching between Migration and Invadopodia states. Time lapse movie acquired from a Cerulean-Lifeact-H2B-GFP-MDA-MB-231 cell (left) cultured on Alexa 488-gelatin (right). Centroid tracking is shown in blue and invadopodia are denoted by red circles (Starting at 110, 370 and 520 min). Time between frames: 10 minutes. Scale bar 10 μm.

Supplementary Movie 3. Oscillations of cortactin fluorescent signal in invadopodia

Representative example of time lapse recording of Cerulean-cortactin-MTLn3 cells (left) on gelatin with 0.39 cross-linking degree, used for cortactin oscillation measurements in **Figure 4B**. The cortactin punctae were filtered by Laplacian of Gaussian filter (right, Log 3d). Inserts zoom-in to an individual invadopodium. Time between frames: 30 seconds. Scale bars are 10 μm in the left and right panels and 5 μm in the inserts.

Supplementary Movie 4. Absence of cortactin oscillations upon F-actin polymerization inhibition by Cytochalasin D.

Representative example of time lapse recording of Cerulean-cortactin-MTLn3 cells (left) cultured on gelatin with 0.39 cross-linking degree and treated with 4 μM Cytochalasin D. Invadopodia precursors, visible as cortactin punctae, were filtered by Laplacian of Gaussian filter (right, Log 3d). Inserts zoom-in to an individual precursor. Time between frames: 30 seconds. Scale bars are 10 μm in the left and right panels and 5 μm in the inserts.

Supplementary Movie 5. Dynamics of calcium spikes measured by Fluo-4-AM.

Representative example of time lapse recording of Cerulean-cortactin-MTLn3 cells on gelatin with 0.39 cross-linking degree. Cells were loaded with Fluo4-AM and used to measure calcium spikes in **Figure 5A-D**. Time between frames: 5 seconds. Scale bar is 10 μm.

Supplementary Movie 6. Dynamics of MT1-MMP vesicle delivery to the plasma membrane.

Representative example of time lapse recording of HS-578T-MT1-MMP-pHluorin cells on gelatin with 0.39 cross-linking degree, used to measure frequency of delivery of MT1-MMP containing vesicles to the plasma membrane in **Figure 5E-G**. Cross-linking degree of 0.39 is shown. Time between frames: 30 seconds. Scale bar is 10 μm.